ISSN 2433-2216(Online)
JAXA-RR-17-010E

JAXA Research and Development Report

Guidance Law Based on Real-time Trajectory Prediction for D-SEND#2

Hirokazu SUZUKI and Tetsujiro NINOMIYA

February 2018

Japan Aerospace Exploration Agency

Contents

Guidance Law Based on Real-time Trajectory Prediction for D–SEND#2

By

Hirokazu SUZUKI[*1] and Tetsujiro NINOMIYA[*2]

Abstract: A flight experiment using a stratospheric balloon, designated as D–SEND#2, was carried out in 2015. This paper describes a guidance law of the D–SEND#2 vehicle. A typical problem of flight experiment using a stratospheric balloon is that it has no nominal trajectory. Therefore, a new real-time trajectory prediction method is devised to overcome this problem. The method solves equations of motion directly for various load factor commands. The guidance law was evaluated using Monte Carlo simulation, and its result was the success rate of 98.1%. The guidance law has a little tolerance to the uncertainty of steady wind and of the model error of C_D because the vehicle has no engine nor devices for velocity control. Actual flight experiments demonstrated that the guidance law satisfied all mission requirements and that it contributed greatly to the mission success.

Keyword: Guidance and Control, Real-time, Trajectory Prediction, D–SEND

Nomenclature

N_z	:	Load factor
C_L, C_D	:	Lift and drag coefficient
C_N	:	Normal force coefficient
G_DP1, G_GM2	:	Guidance parameter
G_RG3, G_h4	:	Guidance parameter
G_Nz4, G_RG4	:	Guidance parameter
L, D	:	Lift and drag
R	:	Range
T_s	:	Time constant for a angle of attack response model
V	:	Velocity

doi: 10.20637/JAXA-RR-17-010E/0001
[*] Received January 30, 2017
[*1] Research and Development Directorate, Research Unit I
[*2] Aeronautical Technology Directorate, Flight Research Unit

$X4F$: Final flight conditions in phase 4

$X5I$: Initial flight conditions in phase 5

g : Gravitational acceleration

h : Altitude

m : Vehicle mass

r : A radius from the center of the Earth to the center of gravity of the vehicle

α : Angle of attack

α_i : Angle of attack command for phase i

γ : Flight path angle

Subscripts

c : Command

1 Introduction

The Japan Aerospace Exploration Agency (JAXA) has conducted a Drop test for Simplified Evaluation of Non-symmetrically Distributed sonic boom (D–SEND) to verify the low boom design using computational fluid dynamics. D–SEND comprises two series of balloon drop tests: D–SEND#1 and D–SEND#2[1)]. For D–SEND#1, an uncontrolled symmetric vehicle was dropped. Then, a controlled experimental low-boom airplane was dropped in D–SEND#2. Both small vehicles achieved supersonic flight without an engine.

Figure 1 presents the D–SEND#2 vehicle configuration. Figure 2 portrays an outline of the flight experiment. The vehicle is dropped from an altitude of 30 km from a stratospheric balloon. The vehicle uses gravity to accelerate to supersonic and passes over a microphone which measures a sonic boom. The measurement system with the microphone for a sonic boom is designated as the Boom Measurement System (BMS)[2)]. The microphone is moored at an altitude of 1 km using a captive balloon to measure the sonic boom, which is not disturbed by

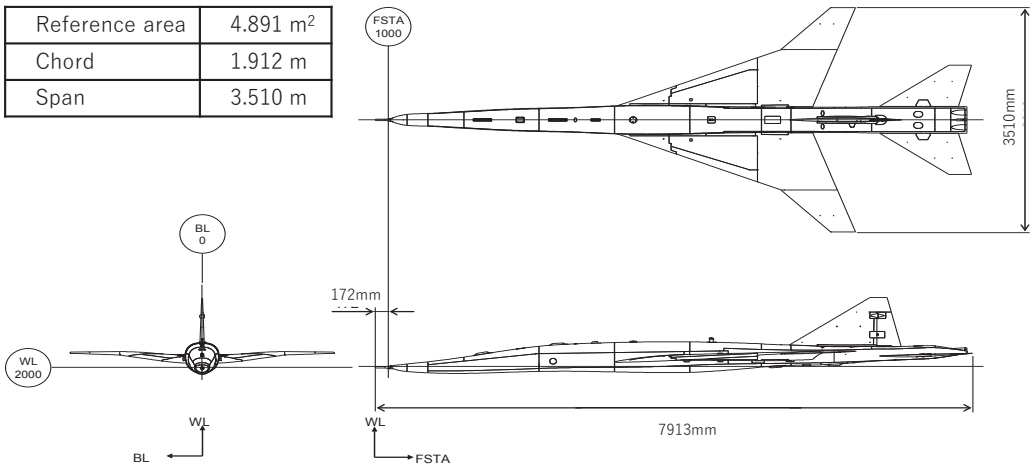

Fig. 1 Three-dimensional configuration.

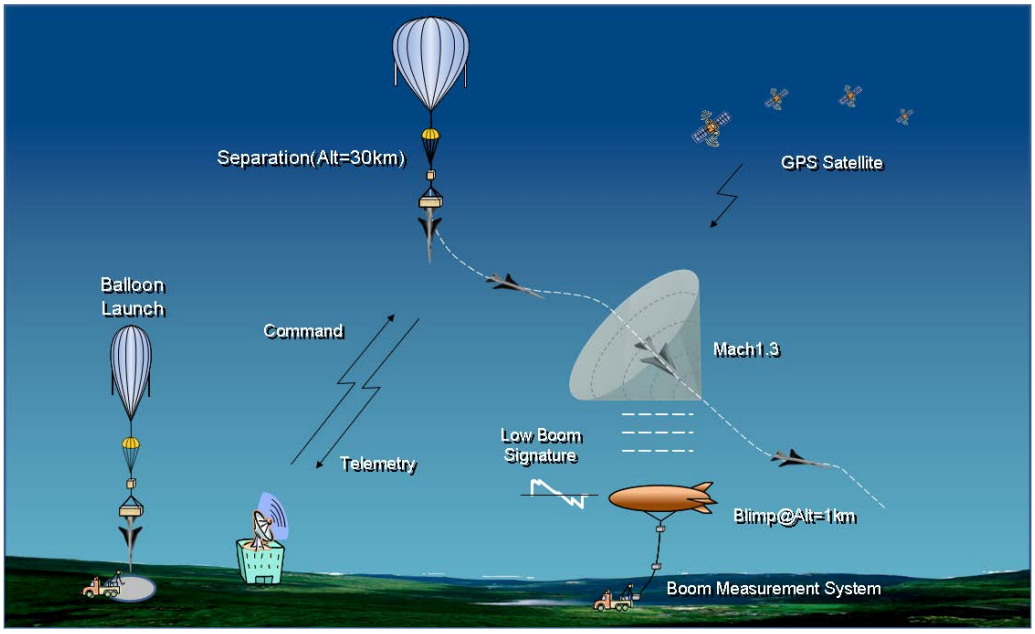

Fig. 2 Summary of flight experiment.

turbulence near the ground.

Only two flight experiments have used a stratospheric balloon for an unmanned supersonic vehicle with guidance and control: the Japanese High-Speed Flight Demonstrator phase–II (HSFD–II)[3] in 2003 and the Italian Unmanned Space Vehicle (USV)[4] in 2010. The main objectives of these flight experiments were the measurement of its aerodynamic characteristics by an α-sweep maneuver for maintaining the Mach number during flight. The position for measurement was not prescribed because measurements were taken by on-board sensors.

The main objective of D–SEND#2 is to measure a sonic boom by the BMS from the ground. Because the stratospheric balloon has no device for controlling its position within the horizontal plane, one BMS is selected from three BMSs set up in the flight test area after the separation. Therefore, the vehicle must establish a desirable flight condition above the BMS from the separation point, which cannot be prescribed beforehand. Hence, the vehicle must satisfy both requirements of flight conditions above the BMS and those of precise guidance for the BMS position at the same time.

This paper presents a specific examination of a guidance law of D–SEND#2 vehicle. The most important requirements for the guidance law are the following.

A) The guidance law must be processed by an on-board computer within a 10 Hz cycle.

B) The guidance law must adjust to an extremely wide separation space because the separation position can not be prescribed.

C) The guidance law has no nominal trajectory. Therefore, even if a proper flight trajectory does not exist in the actual flight, the guidance law must output some preferred commands.

The guidance law comprises two main logics to adjust those requirements. The first logic outputs some commands based on previously designed flight trajectory data, to adapt A) and B). These trajectories are

named as reference trajectories. The second logic is devised to overcome B) and C). It is based on a real-time trajectory prediction. The method obtains various trajectories from solving the equations of motion directly by inputting the load factor command as a parameter. The method selects the most desirable trajectory from them. Solving the equations of motion overcomes C). It has another benefit: constraints such as dynamic pressure or load factor can be dealt with directly. When the trajectory does not meet with those constraints, it is rejected. If all the trajectories do not satisfy the requirements, then the most preferred trajectory can be selected.

The Esrange Space Center in Sweden was selected as the flight experiment site. Because the BMS must be set on the ground, other candidates were rejected. The flight test field is designated as Zone B (see Fig. 7).

2 Guidance Law

2.1 Overview

Measurement requests of flight conditions at the sonic boom generation are presented in Table 1. Constraints for flight trajectory are the followings.

- Dynamic Pressure $< 65\,\mathrm{kPa}$
- Load Factor $< 4.5\,\mathrm{G}$

The guidance law must satisfy the measurement requests and the constraints of actual flight. The guidance law comprises two logics. The first logic outputs the guidance commands based on the trajectory data to the

Table 1 Requirements for sonic boom measurement.

Item	Requested Accuracy
Mach number	1.3±0.1
Rate of change of Mach number	0.00±0.01 [1/s]
Lift Coefficient	0.12 (+0.01/-0.02)
Focusing[*1]	[For direct wave[*2]] • If a target sonic boom reaches the BMS faster than the other sonic boom, then the other sonic boom reaches the BMS 0.1 s later than the target boom. • If a target sonic boom reaches the BMS later than the other sonic boom, then the target sonic boom reaches the BMS 0.3 s later than the other sonic boom. [For indirect wave[*3]] • If a target sonic boom reaches the BMS faster than the other indirect wave, then the other indirect wave reaches the BMS 0.1 s later than the target boom. • If a target sonic boom reaches the BMS later than the other indirect wave, then the target sonic boom reaches the BMS 0.5 s later than the other indirect wave.

[*1]:Several sonic booms reach the BMS simultaneously. The BMS can measure eight sonic booms.

[*2]:Direct wave means that it reaches directly to the BMS.

[*3]:Indirect wave means that it reaches to the BMS after reflection from the ground.

Table 2 Flight phases.

No.	Phase	Termination condition	Contents
1	Acceleration	Dynamic pressure $\geq G\_DP1$	Descend with $\alpha_c = 4.5\,\mathrm{deg}$
2	Pull-up	Flight path angle $\geq G\_GM2$	Pull up by $\alpha_c = 12\,\mathrm{deg}$ with N_z limiter
3	Glide	Flight range to the BMS$\leq G_RG3$	Glide with γ_c
4	Dive	Altitude $\leq G\_h4$	Maintain N_{zc}
5	Measurement	Dynamic pressure or altitude or flight path angle, etc	Maintain N_{zc} (equivalent to $C_L = 0.12$)

attitude controller. The second logic outputs the guidance commands based on a real-time trajectory prediction.

Summaries of the reference trajectories were presented in Ref. 5), 6). The flight experiment vehicle is lifted to the altitude of 30 km by a stratospheric balloon. Then it is released with velocity of 0 m/s and a flight path angle of -90 deg. The vehicle must fly with a Mach number of 1.3 and with C_L of 0.12 over the BMS. The most desirable flight condition at the BMS is designated as the target flight condition in this paper. Details of the target flight condition are presented in Ref. 5), 6). The specific conditions are altitude of 7.67 km, Mach number of 1.3, and flight path angle of -45.8 deg. The flight trajectory from separation to the target flight condition is divided into five phases: acceleration, pull-up, glide, dive, and measurement (Table 2). The vehicle must consume the position energy at the separation properly until reaching the BMS. Therefore, minimum and maximum flight range trajectories exist. For the minimum flight range trajectory, the vehicle must consume its surplus initial potential energy until reaching the BMS. For the maximum flight range trajectory, the initial potential energy is equal to the energy necessary for flying to the BMS. An optimal problem is finally composed as follows: the initial conditions are the separation conditions; the final constraints are the target flight conditions, and the performance index is the flight range. Thus, reference trajectory data are calculated from optimization process for various initial conditions. The guidance commands based on the reference trajectory data are outputted in all phases except for dive phase.

The guidance law based on the real-time trajectory prediction is used in the dive phase to compensate for the model errors and the uncertainties related to the actual flight conditions.

Details of the guidance law are presented hereinafter.

2.2 Acceleration Phase

The vehicle accelerates with a constant angle of attack command of 4.5 deg, which is the same setting as in the optimal problem.

A guidance law parameter of G_DP1 is calculated once at the separation, and the flight phase goes to the next phase when the dynamic pressure exceeds G_DP1. From the obtained trajectory data, G_DP1 is formulated as a function of the flight range as is shown in Fig. 3.

2.3 Pull-up Phase

The guidance law outputs the constant angle of attack command of 12.0 deg, which is also the same setting as the optimal problem. The angle of attack command is overwritten by the limiter to prevent the vehicle from exceeding the load factor limit if the load factor reaches 3.5 G. Details of the limiter logic are presented in Ref. 6).

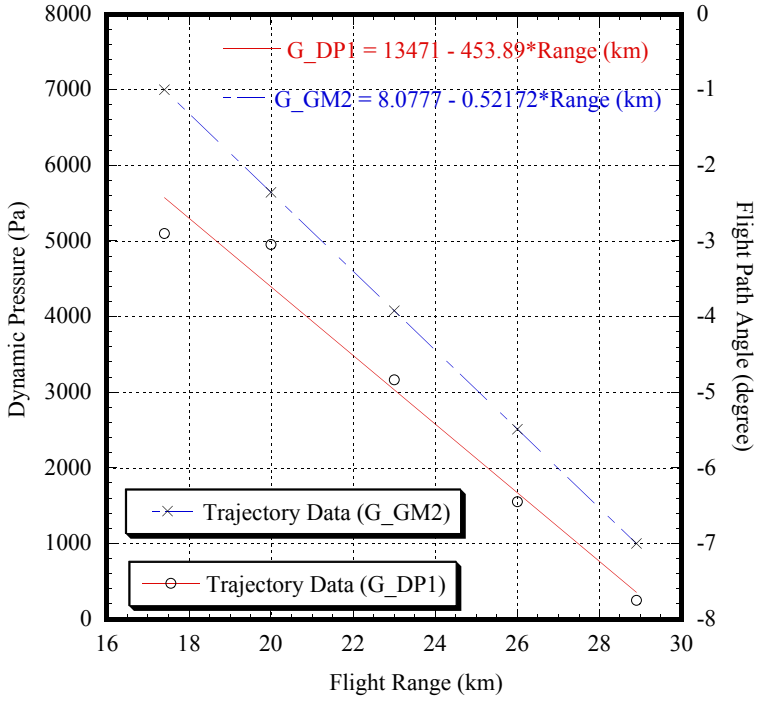

Fig. 3 G_DP1 and G_GM2. Both are defined by polynomials of the flight range.

When the flight path angle reaches G_GM2, the flight phase changes. Figure 3 also shows G_GM2 which is formulated as similar to G_DP1.

2.4 Glide Phase

The guidance law outputs a flight path angle command, which is formulated as three parts of polynomial expressions of kinematic energy as shown in Fig. 4. The flight path angle command is made for typical flight ranges. Figure 4 shows the maximum flight range case.

The glide phase is ended when the range-to-go reaches G_RG3, which is a function of the altitude of separation. This parameter is calculated by linear interpolation using the parameter values in Table 3.

2.5 Dive Phase

Although the guidance law outputs the commands based on the obtained trajectory data during the previous flight phases, it must compensate for the model errors and the uncertainties related to the actual flight conditions.

Table 3 G_RG3 and G_RG4.

Altitude (km)	G_RG3 (km)	G_RG4 (km)
26	5.679	3.860
27	5.660	3.824
28	5.815	3.986
29	6.153	4.322
30	5.958	4.130
31	5.952	4.123

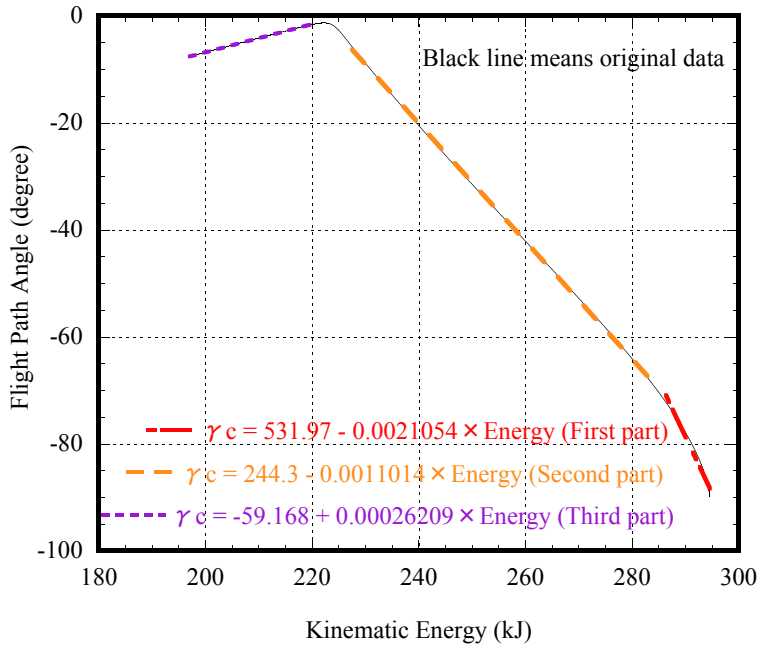

Fig. 4 Gamma command is defined by a series of polynomials of kinematic energy.

The guidance law based on the real-time trajectory prediction method serves this role.

Real-time trajectory prediction performed at the first cycle of this phase determines the load factor command (G_Nz4) and the final altitude of this phase (G_h4). When the altitude becomes less than G_h4 the dive phase is finished.

Figure 5 presents the concept of the method. On the one hand, the motion prediction function calculates the final flight conditions of the dive phase($X4F$) by integrating the equations of motion from the present flight conditions to the flight range of G_RG4 with a constant load factor of N_{zc}. On the other hand, $X5I$ expresses a set of initial conditions of the measurement phase that satisfy the measurement conditions of Table 1 when the vehicle flies with C_L of 0.12 from these initial conditions to a BMS and $X5I$ is expressed using a plane equation. Therefore, if $X4F$ calculated using a certain load factor command satisfies $X5I$, the vehicle will satisfy the measurement conditions naturally. Then the vehicle flies with the load factor during the dive phase and glides with C_L of 0.12 during the measurement phase.

Firstly, the contents of the motion prediction are described. During the dive phase, the attitude controller maintains the bank angle of 0 deg in order to avoid interaction between the lateral motion and the longitudinal motion and to prepare for the sonic boom measurement. Therefore, the motion prediction is performed only for longitudinal motion. The independent variable is the flight range instead of time. Two reasons exist for this formulation. If the flight range is selected as the independent variable, then the $X4F$ that is the integrated value from the present flight condition to the flight range of G_RG4 is obtained exactly. The other reason is to reduce the computational cost by eliminating one variable of time. The state vectors are altitude, velocity, flight path angle, and angle of attack. The control variable is the angle of attack command, and the independent variable is the flight range. The equations of motion are as follows;

$$\frac{dh}{dR} = \tan\gamma \tag{1}$$

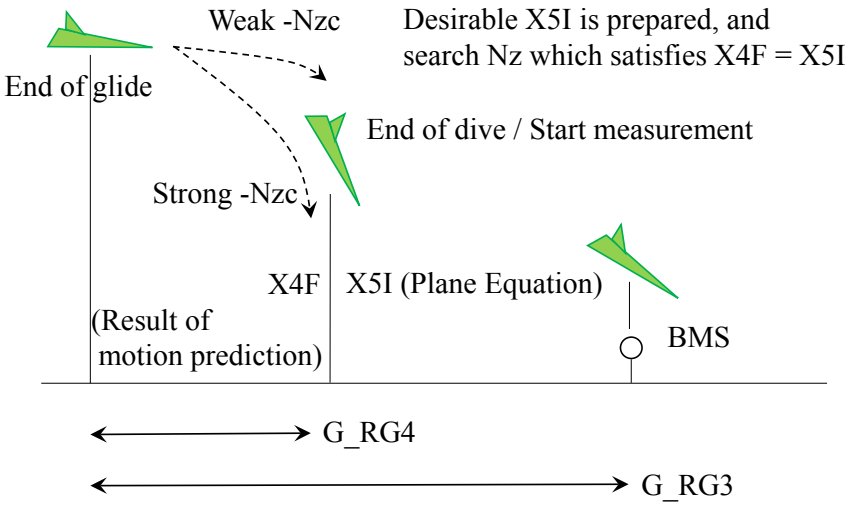

Fig. 5 Concept of real-time trajectory prediction method.

$$\frac{dV}{dR} = \frac{-D/m - g\sin\gamma}{V\cos\gamma} \tag{2}$$

$$\frac{d\gamma}{dR} = \frac{L/(mV) + (V/r - g/V)\cos\gamma}{V\cos\gamma} \tag{3}$$

$$\frac{d\alpha}{dR} = \frac{\alpha_c - \alpha}{T_s V\cos\gamma} \ . \tag{4}$$

The angle of attack is modeled as controlled by the angle of attack command[5, 6]. This equation of angle of attack response is formulated using a first-order delay model with a time delay based on the attitude controller performance. Then the time constant T_s is 1.28 s; the time delay is 0.6 s.

The final state of the dive phase, $X4F$, is obtained by integrating from the present condition to the flight range of G_RG4.

Secondly, the approach of formulating of the $X5I$ plane is described. The following initial conditions at the beginning of measurement phase are presumed: the altitude is 8–14 km; the velocity is 300–460 m/s, and the flight path angle is -90 deg to 0 deg. These ranges are set sufficiently wide based on the previous investigation. Their intervals are, respectively 100 m, 1 m/s, and 1 deg. The angle of attack is the same value of the angle of attack command and it is 4.2598 deg, corresponding to C_L of 0.12 at Mach number of 1.3 in all cases. The flight simulations are conducted for all combinations of the initial conditions, and the area where measurement of the sonic boom is acceptable was investigated. The combinations of initial conditions are then selected so that the desirable sonic boom reaching the area has a width of ±2 km from the BMS. The plane equation of $X5I$ is formulated as including those combinations of initial conditions. Figure 6 shows a sample figure of $X5I$ plane. Each pair of red and yellow solid lines in Fig. 6 show the contour lines of the desired sonic boom propagation area for an initial altitude case. Red solid lines show the contours for the desired sonic boom propagates 2 km. The yellow lines show those for 3 km. The green dotted lines show the approximated linear lines of contours of every altitude. The plane equation of $X5I$ is formulated by including these approximated linear lines and is

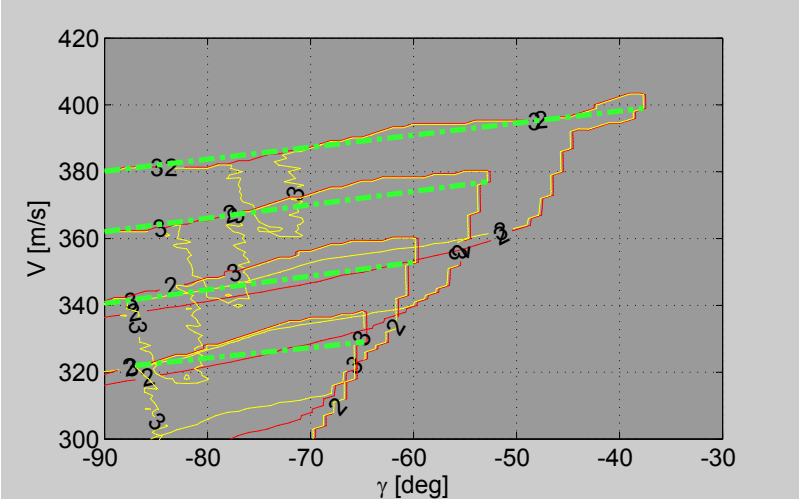

Fig. 6 Example of X5I plane.

expressed as;

$$2.4301 \times 10^{-2}h - 5.0245 \times 10^{-4}\gamma + 1.8443 \times 10^{-3}V = 1. \tag{5}$$

Finally, the real-time trajectory prediction method is applied as shown below, where the guidance parameter G_RG4 is calculated by linear interpolation using the parameter values in Table 3.

Step 1) An initial value of G_Nz4 is set from 0 G to -4.0 G every 0.1 G.

Step 2) The final state, $X4F$, is calculated by integrating the equations of motion from the present states to the flight range of G_RG4 with given G_Nz4.

Step 3) The points of intersection between $X4F$ and $X5I$ are calculated.

Step 4) Go to Step 1) and change G_Nz4. If G_Nz4 reaches -4.0 G, then go to Step 5).

Step 5) If several intersection points exist, then G_Nz4 such that γ of $X4F$ is the nearest to the target flight path angle ($= -60$ deg) is selected. If there is no intersection, a minimum distance between $X4F$ and $X5I$ plane case is selected.

2.6 Measurement Phase

The guidance law outputs N_{zc} to establish target C_L, where N_{zc} is calculated using dynamic pressure measured by an air data sensor and corresponds to C_L of 0.12.

3 Evaluation of Performance

3.1 Presumed Conditions

Evaluation of the guidance law is performed by the simulations of motion of 3 degrees of freedom and by supporting the vehicle as a point of mass. The only control variable is the angle of attack command. The states are altitude, velocity, the flight path angle, the heading angle, latitude, longitude, and the angle of attack. This paper does not address lateral guidance because it is regarded as an aspect of the attitude control. The vehicle

Table 4 Model errors and uncertainties.

Item	Value*1	Distribution
Separation altitude	28–30 km	uniform
Separation pitch angle	-88.6 ± 2 deg	normal
C_L	Depends on Mach number	normal
C_D	Depends on Mach number	normal
Atmosphere	Depends on altitude	normal
Steady wind	Depends on altitude	normal
T_s	$\pm 10\%$	normal
Separation position	Inside of permitted separation area and desirable separation area*2	uniform

*1: The value indicates $\pm 3\sigma$ value for a normal distribution and maximum/minimum values for a uniform distribution.

*2: See Fig. 7 and Fig. 10

is controlled by adjusting the direction of its vertical fin to the BMS during the acceleration phase. If this maneuver is controlled well, then the vehicle can fly straight to the BMS after pulling up. The control logic of the direction of the vehicle's fin is designated as an initial roll control. Although this control logic uses Euler angles, the Euler angles cannot be defined in a 3 degree of freedom simulation. Therefore, this study does not examine lateral guidance and presumes that the initial roll control is performed well. Details of the initial roll control are described in Ref. 7).

Although steady winds are assumed for the flight simulation, the bank angle command is constantly set as 0 deg. Aerodynamic coefficients are modeled as a trimmed C_L and C_D[6]. Judgment for the requirements shown in Table 1 is evaluated using ray path analysis[8].

3.2 Error Models

Error models and its related values are presented in Table 4.

3.3 Monte Carlo Simulation (MCS)

The distribution of separation points is portrayed in Fig. 7. Its vertical axis and horizontal axis respectively represent south-north and east-west. Wherever the vehicle is separated from the area defined in Table 4, it selects one of BMS and must generate a desired sonic boom above the BMS. 'Desirable separation area' in Table 4 is defined as follows; The vehicle can fly a certain range of distance which is determined by the separation altitude, as is shown in section 2.1. Therefore, if the separation altitude is given, the minimum and maximum distance of this achievable range of distance can be obtained. The intermediate distance of concentric circle with this minimum and maximum distance from each BMS is 'Desirable separation area'.

With random combinations of errors shown in Table 4, 1 000 flight simulation cases were conducted. Results of the flight simulations were checked first for whether they satisfy the constraints. If it exceeds the limitation of dynamic pressure or the load factor, then it is categorized as a 'violation'. If it satisfies all constraints, it is evaluated then whether the measured sonic boom at the BMS satisfies the requirements presented in Table 1. The result is classified as a 'mission failure' if the sonic boom does not satisfy all requirements. It is a 'success' case if it is not defined as a 'violation' or 'mission failure'. As a result of the MCS, the success case is 981 cases.

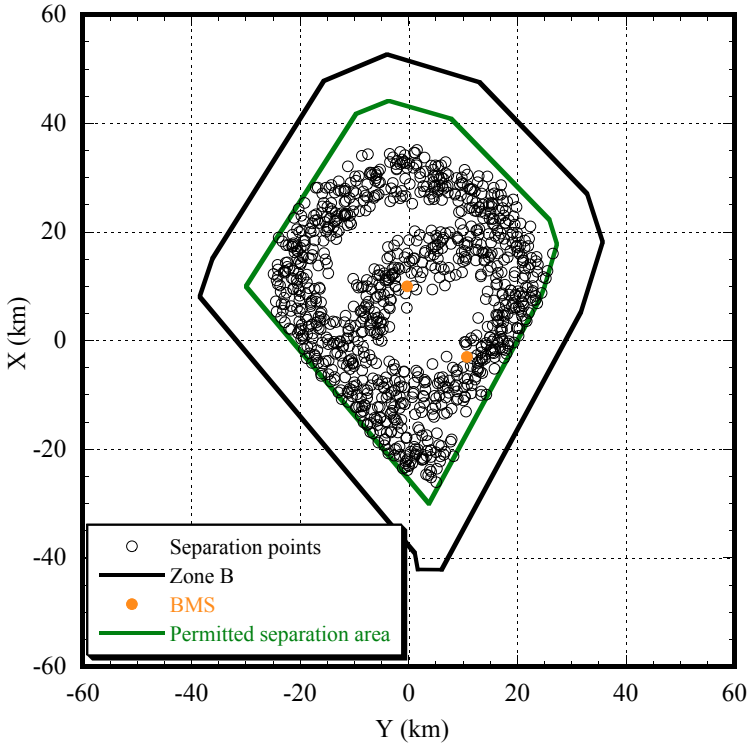

Fig. 7 Distribution of separation points in MC.

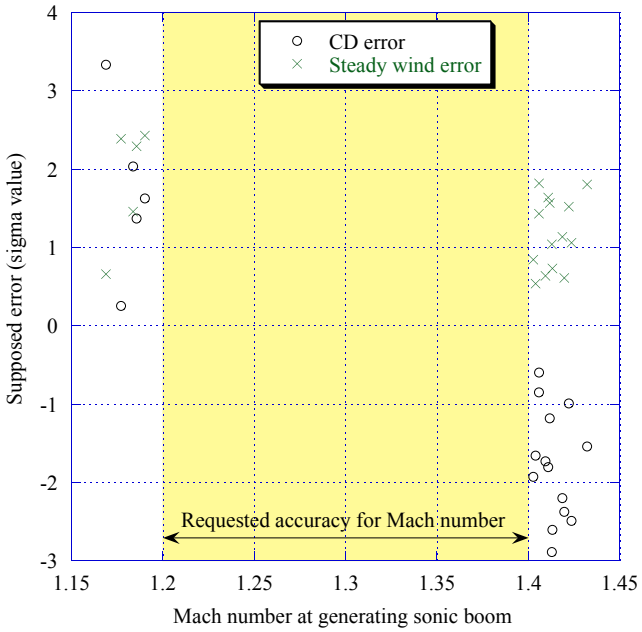

Fig. 8 Measured Mach number of mission failure case.

The mission failure cases are 19 cases. All mission failure cases violated the Mach number requirement. No boom focusing case occurred. The success rate requirement to the guidance and control system is 90 %. This success rate for the guidance law was accepted, because there are no device to control vehicle's velocity.

Figure 8 shows the relation between the Mach number at the generation of a measured sonic boom and

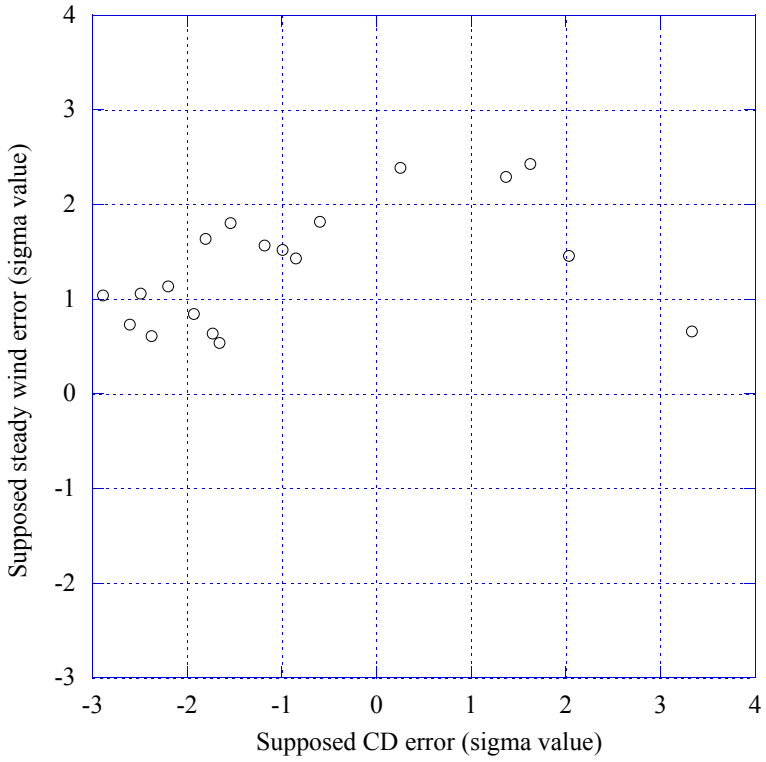

Fig. 9 Set values of steady wind and C_D.

typically presumed error values of the mission failure cases. It shows a trend by which the Mach number is below the requirement in case of a positive C_D error, and the Mach number exceeds the requirement in case of a negative C_D error. Figure 9 depicts C_D error and steady wind error of the mission failure cases. It shows a trend by which the steady wind error becomes large in case of a small absolute value of C_D error.

Figure 10 shows separation points of mission failure cases. Although they show a weak trend by which failure cases concentrate around the longer range and higher altitude, they spread widely in the desired separation area.

4 Result of Actual Flight

The flight experiment was conducted on July 24, 2015. Evaluations by actual flight results are presented herein.

During flight campaign in 2014, there were no suitable day for flight test. After this campaign, separation condition was expanded after precise investigation. As a results, the upper bound of desirable separation area was extended from 30 km, as shown in Fig. 10, to 33 km, as shown in Fig. 11.

4.1 Actual Flight Trajectory

The vehicle was released within an extended separation area (Fig. 11), and it flew straightly towards a selected BMS (Fig. 12). Figure 13 shows the actual flight trajectory with Mach number and an altitude. The actual flight trajectory is accompanied with a predicted trajectory with no error and a simulated trajectory with C_D having -3 σ error. In these trajectories, the initial altitude is the output of EGI (Embedded GPS/INS), and Mach number is that of ADS (Air Data Sensor). The simulated trajectory shows good correspondence with the actual one. The aerodynamic coefficients were estimated in the post-flight analysis, and the estimated C_D is

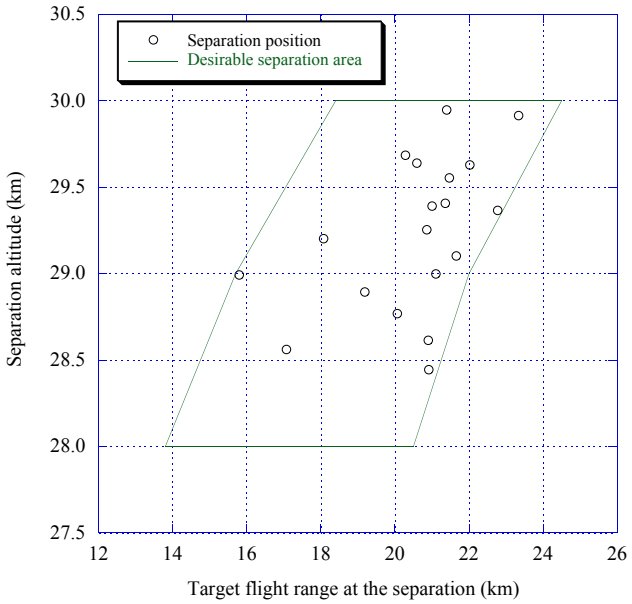

Fig. 10 Separation positions of mission failure cases.

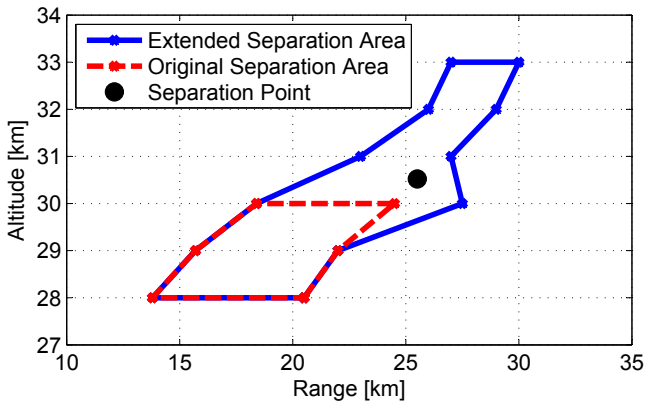

Fig. 11 Actual separation point.

shown in Fig. 14. As Fig. 14 shows C_D has a large error, and this error was almost equivalent to -3 σ value.

4.2 Conputational Load on On-board Flight Computer

The CPU of the on-board flight computer is Power PC, MPC7410, and its clock frequency is 400 MHz. The guidance law task was a 10 Hz cycle. All calculations were performed within the cycle.

4.3 Acceptance for Required Conditions

The maximum dynamic pressure was 57.26 kPa. The respective maximum and minimum load factors were +3.72 G and -3.89 G.

Flight conditions of the measured target sonic boom were estimated as a Mach number of 1.386, change rate of Mach number within $\pm 0.005\,\mathrm{s}^{-1}$, and C_L of 0.122.

Therefore, the guidance law satisfied all the requirements.

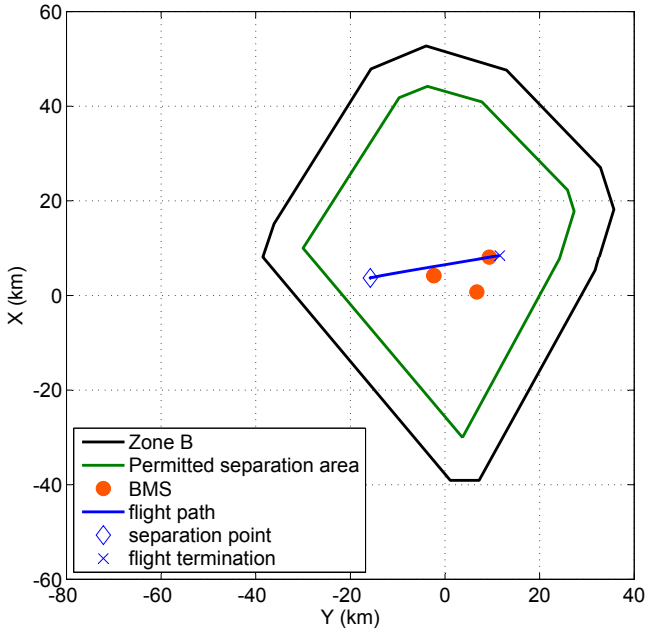

Fig. 12 Flight path in horizontal plain.

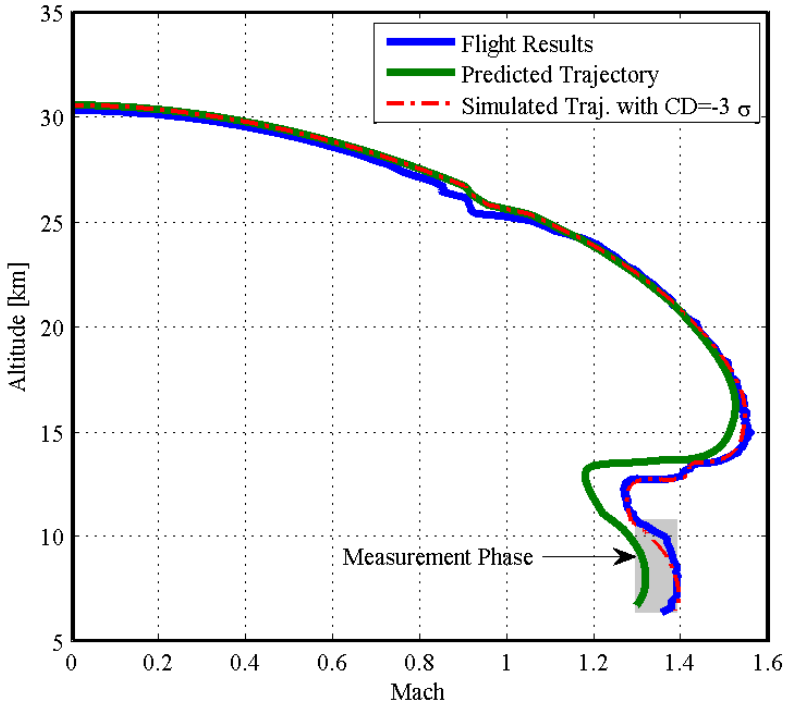

Fig. 13 Actual flight trajectory.

4.4 Results of Real-Time Trajectory Prediction Method

The actual value of guidance parameters are aummerized in Table 5. The flight phase proceeded properly from the dive phase to the measurement phase at the altitude of G_h4.

As Fig. 14 shows, the estimated C_D is close to the assumed minimum value. Therefore, actual flight

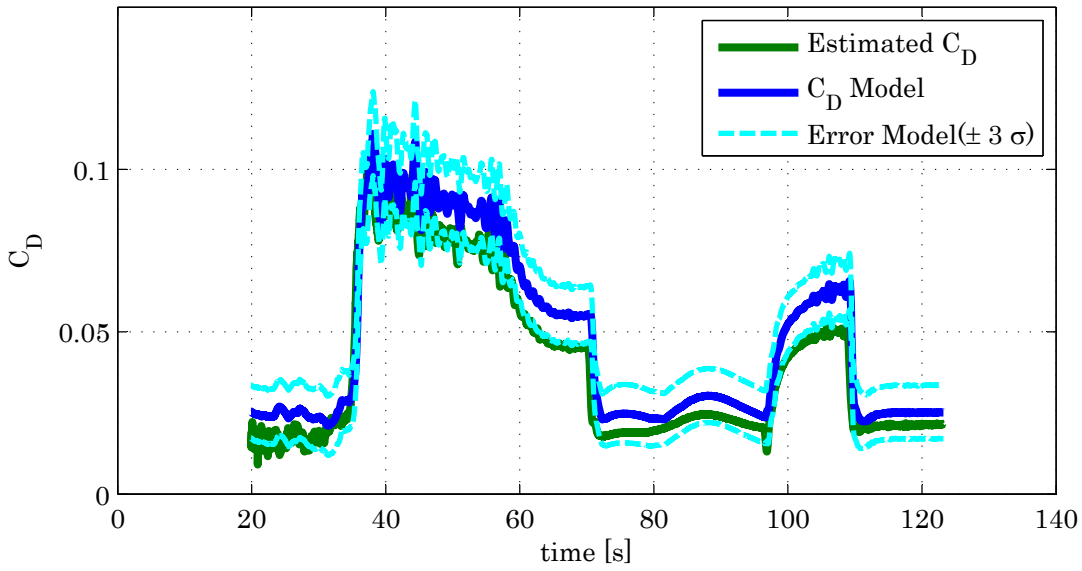

Fig. 14 Estimated drag coefficient.

Table 5 Guidance parameters used in the actual flight.

Item	Value
G_DP1	2 408.9 Pa
G_GM2	-4.26 deg
G_RG3	5 954.9 m
G_h4	10 875.9 m
G_N4	-2.9 G
G_RG4	4 126.4 m

experiments must be the most difficult condition for the vehicle which has no effector for velocity control. Nevertheless, the guidance law worked extremely well, leading to complete success.

From the viewpoint of managing risks, although C_D is a parameter sensitive to the mission success, C_D estimated from the actual flight data was significantly differenet from model value. This implies that the simulation model including error models was not as accurate as expected, and margin to mission success was not satisfactory.

5 Conclusions

This paper reported the guidance law of D–SEND#2. The guidance law used some trajectory data to realize a desirable trajectory for an actual flight. Furthermore, the real-time trajectory prediction method was devised to achieve all mission requirements against mathematical model errors and uncertainties.

The guidance law was evaluated using MCS, and the result was the success rate of 98.1%. Results clarified that the guidance law has a little tolerance to the uncertainty of steady wind and of the model error of C_D because the vehicle has no engine or devices for velocity control.

Results of evaluation for guidance law using actual flight data show that the real-time trajectory prediction was accomplished within the performance of the on-board computer. Although the drag coefficient model was

estimated to be close to the presupposed minimum value, the guidance law realized a successful flight in which all mission requirements are satisfied. On the other hand, this results direclty require that future works should include enhancing the model building accuracy.

References

1) Honda, M. and Yoshida, K., D–SEND Project, Aeronautical and Space Sciences JAPAN, No.60 (2012), pp. 245-249 (in Japanese).

2) Kawakami, H., Shindo, S. and Naka, Y., Development and Operation of Sonic Boom Measurement System in D–SEND#1, Aeronautical and Space Sciences JAPAN, No.61 (2013), pp. 1-7 (in Japanese).

3) Yanagihara, M. et al., Results of High Speed Flight Demonstration Phase II, Proceedings of the 55th International Astronautical Congress, IAC-04-V.6.03, Vancouver, Oct. 2004.

4) Matteis, P. et al., The Italian Unmanned Space Vehicle FTB-1 Back to Fly, Experimental Objectives and Results of the DTFT-2 Mission, Proceedings of the 61th International Astronautical Congress, IAC-10.D2.6.7, Prague, Sep. 2010.

5) Suzuki, H. and Tomita, H., Optimal Trajectory Design for D–SEND#2 Vehicle, Proceedings of the 14th Australian International Aerospace Congress, Melbourne, Feb. 2011.

6) Suzuki, H., Trajectory Design of D–SEND#2, JAXA Research and Development Report, JAXA-RR-15-002, 2015 (in Japanese).

7) Ninomiya, T., Suzuki, H. and Kawaguchi, J., Controller Design for D–SEND#2, Proceedings of the 3rd CEAS Euro GNC conference, Toulouse, April. 2015.

8) TAKAGI, S., SUZUKI, S., and YOSHIKAWA, A., Ascent Trajectory Optimization Considering the Sonic Boom, Journal of the Japan Society for Aeronautical and Space Sciences, No.48 (2000), pp405–410 (in Japanese).

JAXA Research and Development Report JAXA-RR-17-010E

Guidance Law Based on Real-time Trajectory Prediction for D-SEND#2

Edited and Published by: Japan Aerospace Exploration Agency
7-44-1 Jindaiji-higashimachi, Chofu-shi, Tokyo 182-8522 Japan
URL: http://www.jaxa.jp/
Date of Issue: February 22, 2018
Produced by: Matsueda Printing Inc.